Bollettino Unione Matematica Italiana

L. Beirão da Veiga

A Local Error Estimator for the Mimetic Finite Difference Method

Bollettino dell'Unione Matematica Italiana, Serie 9, Vol. **1** (2008), n.2, p. 319–332.

Unione Matematica Italiana

<http://www.bdim.eu/item?id=BUMI_2008_9_1_2_319_0>

Bollettino dell'Unione Matematica Italiana, Unione Matematica Italiana,
2008.

Bollettino U. M. I.
(9) **I** (2008), 319-332

A Local Error Estimator for the Mimetic Finite Difference Method (*)

L. Beirão da Veiga

Abstract. – *We present a local error indicator for the Mimetic Finite Difference method for diffusion-type problems on polyhedral meshes. We prove the global reliability and local efficiency of the proposed estimator and show its practical performance on a standard test problem.*

1. – Introduction.

The Mimetic Finite Difference method has been applied successfully in a large range of applications, for instance electromagnetics, gas dynamics and diffusion. The advantage of such a method is twofold. First, it allows for a large choice of discrete scalar products, leading to an entire range of different (consistent and stable) numerical schemes for the same problem. This additional freedom can be used, for instance, to tackle a scheme which satisfies some additional physical or numerical properties. Second, the Mimetic Finite Difference method allows for general polyhedral meshes with degenerate and non-convex elements, which is a very useful property in many applications.

In the present paper we consider the diffusion problem written as a system of two equations

$$
\begin{aligned}
&\mathrm{div}\, \boldsymbol{F} = b\ , \qquad \boldsymbol{F} + \mathbb{K}\boldsymbol{\nabla} p = 0 && \text{in } \Omega \\
&p = 0 && \text{on } \partial\Omega\ .
\end{aligned} \tag{1}
$$

The first equation represents the mass conservation while the second one is the constitutive equation relating the scalar variable p to the velocity field $\boldsymbol{F}$ through the symmetric material tensor $\mathbb{K}$. For simplicity, we consider the case of homogeneus Dirichlet boundary conditions for the scalar variable.

The diffusion problem has already been the object of a large number of papers in the literature of MFD, see for example [6, 7, 19, 20, 21, 22, 23, 25, 26] and

(*) Comunicazione tenuta a Bari il 26 settembre 2007 in occasione del XVIII Congresso dell'Unione Matematica Italiana.

references therein. In [11, 13], the authors proved for the first time the convergence of the method for general polyhedral unstructured meshes with flat and curved faces, while in [12] a family of inexpensive MFD discretization schemes was introduced.

As noted above, one of the main advantages of the MFD method with respect to classical finite elements is the generality of the mesh. The elements can be general degenerate and non-convex polyhedrons, eventually of different type across the domain. Such flexibility makes the MFD method a very appealing ground for the application of adaptive strategies for error control. In the present paper we present a local (reliable and efficient) residual-based error estimator for the MFD method applied to problem (1). In this contribution we therefore focus on the evaluation of the local error, which is a key issue in adaptivity. The results of this paper are shown without proof; the proofs can be found in [4, 5].

The paper is organized as follows. In Section 2, we briefly review the Mimetic Finite Difference method and, in particular, the assumptions on the scheme. We essentially require the same (minimal) properties on the mesh geometry and discrete scalar products introduced in [11] to prove the convergence of the method. Moreover, we introduce a post-processing scheme for the scalar variable, in the spirit of [27, 24]. The post-processed pressure is shown to converge in a stronger norm and it is a key ingredient in the proposed error estimator. Afterwards, in Section 3 we introduce the local error indicator, and show the main result of the paper, i.e. global reliability and local efficiency bounds. Finally, in Section 4 we combine our error estimator with an adaptive strategy and apply it to a standard benchmark problem, in order to show the practical performance of the error indicator. More numerical tests can be found in [5].

In the whole contribution the scalar C will indicate a general positive constant, eventually different at each occurrence, uniform in the mesh size.

REMARK 1.1. – For simplicity of exposition, in the present paper we focus the proofs and notation on the case of three dimensional problems. The error estimator for the bi-dimensional case is identic, the proofs being a simpler reformulation.

2. – The mimetic finite difference method.

In the present section we give a brief description of the Mixed Finite Difference method applied to problem (1).

Let Ω be a polyhedron with Lipschitz continuous boundary. Furthermore, let Ω_h be a non-overlapping conformal partition of Ω into simply-connected polyhedral elements with flat faces. We indicate in the sequel the set of faces of Ω_h with $\mathcal{E}_h$, and with h_E the diameter of each element E. Furthermore, for every

$E \in \Omega_h$ and every face $e \in \partial E$, let $\boldsymbol{n}_e^E$ represent the outward unit normal to e. Moreover, in the sequel we associate to every $e \in \mathcal{E}_h$ a normal unit vector $\boldsymbol{n}_e$, fixed once and for all.

We assume the following properties of the mesh Ω_h, introduced in [11] in order to derive the a priori error converge estimates for the scheme.

(M2) We assume that we have two positive integers N_e and N_l such that every element E has at most N_e faces, and each face e at most N_l edges.

(M3) We assume that there exist three positive constants v_*, a_* and l_* such that for every element E it holds

$$v_* h_E^3 \leq |E| \ , \quad a_* h_E^2 \leq |e| \ , \quad l_* h_E \leq |l|$$

for all faces e and edges l of E, where here and in the sequel $|E|, |e|, |l|$ represent respectively the volume of E, the area of e and the length of l.

(M4) We assume that the mesh faces are flat and that there exists a positive number γ_* such that: for each element E and for each face $e \in \partial E$ there exists a point $M_e \in e$ such that e is star-shaped with respect to every point in the disk of center M_e and radius $\gamma_* h_E$.

(M5) We further assume that for every $E \in \Omega_h$, and for every $e \in \partial E$, there exists a pyramid P_E^e contained in E such that its base equals to e, its height equals to $\gamma_* h_E$ and the projection of its vertex onto e is M_e.

(M6) We assume that there exists a positive number τ_* such that: for each element E there exists a point $M_E \in E$ such that E is star-shaped with respect to every point in the disk of center M_E and radius $\tau_* h_E$.

In the sequel, we assume for simplicity that the tensor field $\mathbb{K}$ is piecewise constant with respect to the mesh. In an adaptive framework, since subsequently refined meshes are typically obtained by subdivision, it is sufficient that such assumption holds for the initial mesh.

We also assume the following standard condition.

(P1) The tensor field $\mathbb{K}$ is symmetric and uniformly strongly elliptic, implying that there exist two constants k_* and k^* such that

$$k_* \|\boldsymbol{v}\|^2 \leq \boldsymbol{v}^T \mathbb{K}(\boldsymbol{x}) \boldsymbol{v} \leq k^* \|\boldsymbol{v}\|^2 \qquad \forall \boldsymbol{v} \in \mathbb{R}^3 \ , \forall \boldsymbol{x} \in \Omega \ , \tag{2}$$

where, here and in the sequel, $\|\cdot\|$ indicates the Euclidean norm of $\mathbb{R}^3$. We are now in the position to introduce the Mimetic Finite Difference method.

The *first step* of the MFD scheme is to define the degrees of freedom for the pressure variable p and flux variable $\boldsymbol{F}$. We therefore introduce the space Q^d of discrete pressures that are constant on each element E. For $q \in Q^d$, we denote by q_E its value on E. For notation simplicity, for any $q \in Q^d$, in the sequel we will identify the vector of its values and the respective Ω_h-piecewise constant function.

The space of discrete velocities X^d is defined as follows. To every element $E \in \Omega_h$ and face $e \in \partial E$, we associate a number G_E^e and the respective vector field $G_E^e \boldsymbol{n}_e^E$. We make the continuity assumption

$$G_{E_1}^e = -G_{E_2}^e \tag{3}$$

for each face e shared by two elements E_1 and E_2. Then, the number m of the discrete velocity unknowns will be equal to the number of boundary faces plus twice the number of internal faces. We consider the space X^d as the subspace of $\mathbb{R}^m$ which satisfies (3).

We define the following corresponding *interpolation operators*. Given any function $q \in L^1(\Omega)$, we define its interpolant $q^I \in Q^d$ as

$$(q^I)_E = |E|^{-1} \int_E q \mathrm{d}V \qquad \forall E \in \Omega_h \ . \tag{4}$$

For every function $\boldsymbol{G} \in [L^s(\Omega)]^3$, $s > 2$, with div $\boldsymbol{G} \in L^2(\Omega)$, we define its interpolant $G^I \in X^d$ as

$$(G_E^I)^e = |e|^{-1} \int_e \boldsymbol{G} \cdot \boldsymbol{n}_e^E \mathrm{d}\Sigma \qquad \forall E \in \Omega_h, \ \forall e \in \partial E \ . \tag{5}$$

Note that, in the sequel, there will be no confusion in the notation, because interpolant (4) is applied to scalar functions and interpolant (5) to vector functions.

The *second step* of the MFD method is to build a discrete divergence operator. For each element $\boldsymbol{G} \in X^d$, we define its discrete divergence $\mathcal{DIV}^d \boldsymbol{G}$ as the element of Q^d given by

$$(\mathcal{DIV}^d \boldsymbol{G})_E = |E|^{-1} \sum_{e \in \partial E} |e| G_E^e \qquad \forall E \in \Omega_h \ . \tag{6}$$

It is easy to check that the following very important commuting diagram property holds. For all $\boldsymbol{G} \in [L^s(\Omega)]^3$, $s > 2$, with div $\boldsymbol{G} \in L^2(\Omega)$, it holds

$$\mathcal{DIV}^d \boldsymbol{G}^I = (\operatorname{div} \boldsymbol{G})^I \ . \tag{7}$$

The *third step* of the MFD method is to define scalar products for the spaces Q^d and X^d. For the space Q^d, we take the only consistent choice

$$[p, q]_{Q^d} = \sum_{E \in \Omega_h} |E| p_E q_E \qquad \forall p, q \in Q^d \ . \tag{8}$$

For the space X^d, the scalar product is defined as

$$[\boldsymbol{G}, \boldsymbol{Q}]_{X^d} = \sum_{E \in \Omega_h} [\boldsymbol{G}, \boldsymbol{Q}]_E \qquad \forall \boldsymbol{G}, \boldsymbol{Q} \in X^d \ , \tag{9}$$

where $[\boldsymbol{G}, \boldsymbol{Q}]_E$ is a local scalar product on E. The choice and construction of such local scalar products is a main point in the MFD method, and it is the object of various papers in the literature, see for example [20, 22]. A general procedure for building these products, such that certain fundamental assumptions are satisfied, was given in [12]. We here assume that those same (minimal) stability and consistency assumptions are satisfied.

(S1) There exist two positive constants s_* and S_* such that for every element E in the decomposition we have

$$s_*|E|\sum_{e\in\partial E}(G_E^e)^2 \le [\boldsymbol{G},\boldsymbol{G}]_E \le S_*|E|\sum_{e\in\partial E}(G_E^e)^2 \qquad \forall \boldsymbol{G}\in X^d\ . \tag{10}$$

(S2) For every element E, every linear function q on E and every $\boldsymbol{G}\in X^d$, it holds

$$[(K\boldsymbol{\nabla} q)^I,\boldsymbol{G}]_E = -\int_E q(\mathcal{DIV}^d\boldsymbol{G})_E\,\mathrm{d}V + \sum_{e\in\partial E} G_E^e\int_e q\,\mathrm{d}\Sigma\ . \tag{11}$$

Furthermore, we introduce the local and global norms

$$|||\boldsymbol{G}|||^2_{X^d} = [\boldsymbol{G},\boldsymbol{G}]_{X^d} = \sum_{E\in\Omega_h}|||\boldsymbol{G}|||^2_E\ ,\quad |||\boldsymbol{G}|||^2_E = [\boldsymbol{G},\boldsymbol{G}]_E\ . \tag{12}$$

The *fourth step* of the MFD method is to define the discrete flux operator $\mathcal{G}^d$, as the adjoint of the discrete divergence operator with respect to the introduced scalar products. We have

$$[\boldsymbol{G},\mathcal{G}^d p]_{X^d} = [p,\mathcal{DIV}^d\boldsymbol{G}]_{Q^d} \qquad \forall p\in \boldsymbol{Q}^d\ ,\ \forall \boldsymbol{G}\in X^d\ . \tag{13}$$

Finally, the MFD method for problem (1) reads

$$\mathcal{DIV}^d\boldsymbol{F}_d = b^I\ ,\qquad \boldsymbol{F}_h = \mathcal{G}^d p_d \tag{14}$$

or, in more explicit form,

$$\begin{aligned} &[\boldsymbol{F}_d,\boldsymbol{G}]_{X^d} - [p_d,\mathcal{DIV}^d\boldsymbol{G}]_{Q^d} = 0 && \forall \boldsymbol{G}\in X^d\\ &[\mathcal{DIV}^d\boldsymbol{F}_d,q]_{Q^d} = [b^I,q]_{Q^d} && \forall q\in \boldsymbol{Q}^d\ . \end{aligned} \tag{15}$$

2.1 – *Convergence of the method.*

In [11], the authors prove that properties $(S1)-(S2)$ are implied by the existence of an element lifting operator R_E with certain consistency and stability properties. We here assume the existence of such operator; as underlined in Remark 2.1, this is a very weak assumption. Note that this operator *never needs to be built in practice*, the knowledge of its existence being sufficient for our purposes.

(S) For every element $E\in\Omega_h$ it exists a lifting operator R_E acting on $X^d|_E$, with values in $[L^2(E)]^3$, such that

$$R_E(\boldsymbol{G}_E)|_e \cdot \boldsymbol{n}_e = G_E^e \qquad \forall e \in \partial E$$
$$\text{div } R_E(\boldsymbol{G}_E) = (\mathcal{DIV}^d \boldsymbol{G})_E \qquad \text{in } E \tag{16}$$

for all $\boldsymbol{G} \in X^d$,

$$R_E(\boldsymbol{G}_E^I) = \boldsymbol{G}_E \qquad \forall \boldsymbol{G}_E \text{ constant on } E\ , \tag{17}$$

and the velocity scalar product can be written

$$[\boldsymbol{Q}, \boldsymbol{G}]_E = \int_E \mathbb{K}^{-1} R_E(\boldsymbol{Q}_E) \cdot R_E(\boldsymbol{G}_E) \mathrm{d}V \qquad \forall \boldsymbol{Q}, \boldsymbol{G} \in X^d\ . \tag{18}$$

As shown in [13], the above properties automatically imply the following approximation property

$$\|\boldsymbol{G} - R_E(\boldsymbol{G}^I)\|_{L^2(E)} \le C h_E \|\boldsymbol{G}\|_{H^1(E)} \qquad \forall \boldsymbol{G} \in [H^1(E)]^3\ ,\ \forall E \in \Omega_h\ . \tag{19}$$

In the sequel we will indicate with R the global operator $X^d \to [L^2(\Omega)]^3$, which is obtained combining all the local lifting operators R_E element by element.

The following convergence result for the MFD method is proved in [11].

THEOREM 2.1. – *Assume that the domain Ω is convex and $\mathbb{K} \in W^{1,\infty}(\Omega)$. Let $(\boldsymbol{F}, p)$ be the solution of problem* (1) *and $(\boldsymbol{F}_d, p_d)$ the solution of problem* (15). *Then it holds*

$$\|\boldsymbol{F} - R\boldsymbol{F}_d\|_{L^2(\Omega)} \le C h \|p\|_{H^2(\Omega)}$$
$$\|\text{ div } (\boldsymbol{F} - R\boldsymbol{F}_d)\|_{L^2(\Omega)} = \|b - b^I\|_{L^2(\Omega)} \le C h \|b\|_{H^1(\Omega)} \tag{20}$$
$$\|p^I - p_d\|_{L^2(\Omega)} \le C h^2 (\|p\|_{H^2(\Omega)} + \|b\|_{H^1(\Omega)})\ .$$

Note that the requirements Ω and $\mathbb{K}$ are needed only for $(20)_3$. In the general case, a simple modification of the proof in [11] leads to

COROLLARY 2.1. – *Let $(\boldsymbol{F}, p)$ be the solution of problem* (1) *and $(\boldsymbol{F}_d, p_d)$ the solution of problem* (15). *Let $p \in H^{1+q}(\Omega),\ 0 < q \le 1$. Then it holds*

$$\|\boldsymbol{F} - R\boldsymbol{F}_d\|_{L^2(\Omega)} \le C h^q \|p\|_{H^{1+q}(\Omega)}$$
$$\|p^I - p_d\|_{L^2(\Omega)} \le C h^{s+q} (\|p\|_{H^{1+q}(\Omega)} + \|b\|_{H^1(\Omega)})\ , \tag{21}$$

where $0 \le s \le 1$ is a problem regularity constant, depending on $\mathbb{K}$ and on the shape of Ω.

REMARK 2.1. – In the recent contribution [14], the authors prove that properties (S1) and (S2), under a reasonable algebraic assumption on the discrete scalar product, imply the existence of the local lifting operator R_E. Such a result confirms the general opinion that a "virtual" operator R_E essentially exists in all cases of interest.

Finally, we introduce a post-processing scheme, in the spirit of [27, 24], for the mimetic finite difference method of Section 2 and show a convergence result for the improved solution. The post-processed pressure is used in the computation of the local error estimator of Section 3.

Let the discrete norm

$$|||q|||_{1,d}^2 = \sum_{E \in \Omega_h} \|\nabla q\|_{L^2(E)}^2 + \sum_{e \in \mathcal{E}_h} h_e^{-1} \|[\![q]\!]\|_{L^2(e)}^2 \ , \tag{22}$$

for all q sufficiently regular, where $[\![\cdot]\!]$ represents the classical face jump operator, which is assumed to be equal to the function value on boundary faces. Moreover, let Q_1^d be the space of Ω_h-piecewise linear functions with zero average on each element.

Given $(\boldsymbol{F}_d, p_d)$ solution of problem (15), we define $\bar{p}_d$ as the unique function in Q_1^d that satisfies

$$|E| \nabla \bar{p}_d|_E \cdot \nabla q|_E = -[\boldsymbol{F}_d, (\nabla q)^I]_E \qquad \forall E \in \Omega_h, \ \forall q \in Q_1^d \ . \tag{23}$$

We then set our post-processed pressure as

$$p_d^* = p_d + \bar{p}_d \ . \tag{24}$$

Note that, due to (18) and (17), from (23) it follows

$$\int_E \nabla p_d^* \cdot \nabla q \mathrm{d}V = -\int_E \mathbb{K}^{-1} R_E \boldsymbol{F}_d \cdot \nabla q \mathrm{d}V \qquad \forall E \in \Omega_h, \ \forall q \in Q_1^d \ . \tag{25}$$

We then have the following result. The proof is omitted and can be found in [4]

PROPOSITION 2.1. – *Assume that the domain Ω is convex. Let p_d^* be computed as in* (24), *and* $(\boldsymbol{F}, p)$ *be the solution of problem* (1). *We then have*

$$|||p - p_d^*|||_{1,d} + h^{-1} \|p - p_d^*\|_{L^2(\Omega)} \leq Ch(\|p\|_{H^2(\Omega)} + \|b\|_{H^1(\Omega)}) \ . \tag{26}$$

In the general case of a non convex domain Ω, a simple modification of the proof shows that a weaker convergence result, in the spirit of Corollary 2.1, holds. Note that, due to property (S2), the solution $\bar{p}_d$ of (23) does not depend on the choice for the scalar product $[\cdot, \cdot]_E$.

REMARK 2.2. – An equivalent post-processing for the pressure variable is presented in [15], where the authors focus also on the computational aspects in the calculation of p_d^*.

3. – A local error estimator.

In the present section we introduce a local error estimator, in the spirit of [24], for the mimetic finite difference method under study, and show reliability and efficiency results. Even for the finite element method, local error estimators for the diffusion problem in mixed form are relatively recent, see [8, 16, 24]. For general results regarding a posteriori error analysis, we refer for instance to [28, 1].

Given $(\boldsymbol{F}_d, p_d)$ solution of problem 15, and p_d^* computed as in (24), the proposed error estimator is given by

$$\eta^2 = \sum_{E \in \Omega_h} \eta_E^2 \tag{27}$$
$$\eta_E^2 = |||(\mathbb{K}\boldsymbol{\nabla} p_d^*)^I + \boldsymbol{F}_d|||_E^2 + h_E^2 \|b - b^I\|_{L^2(E)}^2 + \frac{1}{2} \sum_{e \in \partial E} h_e^{-1} \|[\![p_d^*]\!]\|_{L^2(e)}^2 \ .$$

The main result of this contribution is the following Proposition, stating the reliability and efficiency of the proposed estimator. The proof can be found in [4, 5].

PROPOSITION 3.1. – *Let* $(\boldsymbol{F}, p)$ *be the solution of problem* (1). *Then it holds*

$$\|\boldsymbol{F} - R\boldsymbol{F}_d\|_{L^2(\Omega)} + h\| \operatorname{div} (\boldsymbol{F} - R\boldsymbol{F}_d)\|_{L^2(\Omega)} + |||p - p_d^*|||_{1,d} \leq C\eta \ . \tag{28}$$

Moreover,

$$\eta_E \leq C(\|\boldsymbol{F} - R_E\boldsymbol{F}_d\|_{L^2(E)} + h_E\| \operatorname{div} (\boldsymbol{F} - R_E\boldsymbol{F}_d)\|_{L^2(E)} + |||p - p_d^*|||_{1,d,E}) \tag{29}$$

where the norm $|||\cdot|||_{1,d,E}$ *stands for the discrete norm* $|||\cdot|||_{1,d}$ *with the sums restricted to the element* E *and the faces* $e \in \partial E$.

Note that the norm (28) in which we measure the error for the vector variable is essentially equivalent to the $|||\cdot|||_{\text{div}}$ norm adopted in [11], see also remark 3.1 below. Simply, the assumption (S) on the existence of the lifting operator R_E allows us to write it in L^2 form. The a-priori error estimates for the norm in 28 are listed in Theorem 2.1 and Proposition 2.1.

The term $h_E\|b - b^I\|_{L^2(E)}$ appearing in the estimator is not a higher-order term and, in principle, it is not exactly computable. Nevertheless, it can be easily estimated up to higher order terms with a sufficiently high quadrature rule. Finally note that, due to the identity

$$b - b^I = \operatorname{div} (\boldsymbol{F} - R_E\boldsymbol{F}_d) \tag{30}$$

shown in [11], a different scaling can be adopted for the divergence error term and the estimator η easily changed accordingly.

REMARK 3.1. – Assume that $\boldsymbol{F} \in W^{m,q}(\Omega)$ for some $q > 2, 0 < m \leq 1$. Using interpolation properties, inverse inequalities and Lemma 4.1 in [11], it easily follows

$$
\begin{aligned}
|||\boldsymbol{F}^I - \boldsymbol{F}_d|||_{X^d} \leq C_q \Bigg(& h^m |\boldsymbol{F}|_{W^{m,q}(\Omega)} + h^{n(2-q)/2q} \|\boldsymbol{F} - R\boldsymbol{F}_d\|_{L^2(\Omega)} \\
& + \Big(\sum_{E \in \Omega_h} h_E^2 \| \operatorname{div} \boldsymbol{F} - \operatorname{div} R\boldsymbol{F}_d \|_{L^2(E)} \Big)^{1/2} \Bigg)
\end{aligned} \tag{31}
$$

where the constant C_q depends on q and blows up for $q \to 2$. Therefore, even when the lifting operator R is not explicitly known, the first two terms in the norm (28) are important nevertheless. Indeed, it is clear from the previous bound that the convergence of $R\boldsymbol{F}_d$ to $\boldsymbol{F}$ in 28 implies the convergence of $\boldsymbol{F}_d$ to $\boldsymbol{F}^I$ in (31).

4. – A benchmark test.

In this section we address a classical test, the so called L-shaped domain, in order to check the practical performance of the error estimator. A full set of numerical tests, comprising also highly graded loads and jumps in the coefficients, can be found in [5].

We assess the performance of our approach by comparing the error convergence of the numerical approximations that are obtained on given sequences of *uniformly* and *adaptively refined* meshes starting from a given base mesh. The sequence of uniformly refined meshes is built by constructing each mesh by the same mesh generation process used for the base mesh but with finer mesh size parameters. Note that this uniform refinement strategy preserves the conformity and shape-regularity of the mesh. Instead, an adaptively refined

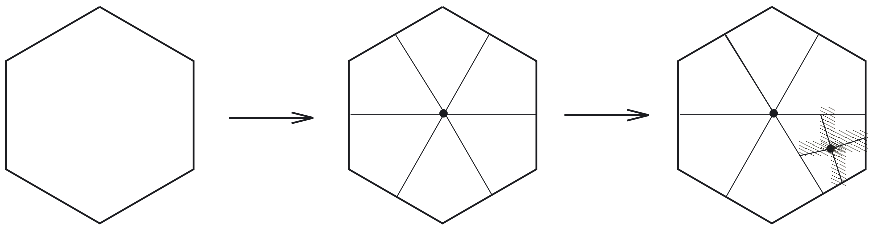

Fig. 1. – Two successive local refinements starting from an hexagonal element.

mesh is generated from a given mesh by refining each element that has been marked for refinement in accordance with the local error estimate provided by our indicator. We adopt a classical marking strategy and refine marked elements E as shown in Figure 1. The details about our marking and refining strategies can be found in [5].

In our test we will present two figures. In the first figure, we display the base mesh from which both uniform and adaptive calculations start, and a locally refined mesh at an intermediate level of the adaptively refinement process. The comparison of the two meshes reflects which part of the computational domain requires refinement according to the error estimator. In the second figure, we show four plots that are labeled from (a) to (d) and that display, respectively,

- (a) the pressure error $||p^I - p_d||_{Q^d}$;
- (b) the flux error $|||\boldsymbol{F}^I - \boldsymbol{F}_d|||_{X^d}$;
- (c) the global error and the global estimator η appearing in Proposition 3.1;
- (d) the effectivity index defined by the ratio between estimator and error.

These quantities are measured on uniformly (solid lines) and adaptively refined meshes (dashes lines) and are plotted versus the total number of mesh elements N. As N is roughly proportional to $1/h^2$ on uniform meshes, the convergence rate of the errors and a-posteriori estimates are reflected by the slopes of the experimental curves shown in the log-log plots (a)-(c). For comparison, in the bottom-left corner of plots (a)-(c) we report the slopes that are expected on the base of "theoretical" arguments. The comparison of the error curves of plots (a)-(b) shows how convergence rates for both pressure and flux (also when the corresponding errors are independently measured) are improved by adapting the mesh according to the a-posteriori estimator η.

The same holds for plot (c) with respect to the target error of Proposition 3.1. Moreover, plot (c) allows the reader to compare the behavior of the error and estimator, see again Proposition 3.1. Finally, the effectivity index shown in plot (d) highlights the precision of the global estimator in the evaluation of the global error. For computational convenience, we approximate the term $||\boldsymbol{F} - R\boldsymbol{F}_d||^2_{L^2(\Omega)}$ by $\sum_E |||\boldsymbol{F}^I - \boldsymbol{F}_d|||^2_E$.

4.1 – *The L shaped domain test.*

We consider the Poisson problem on a L-shaped domain, obtained carving out the lower right quarter from the square domain $[-1, 1]^2$. The source term b is null, and the boundary conditions are set in accordance with the pressure solution

$$p(r, \theta) = r^{2/3} \sin(2\theta/3), \tag{32}$$

here expressed in terms of the polar coordinates (r, θ) in the plane.

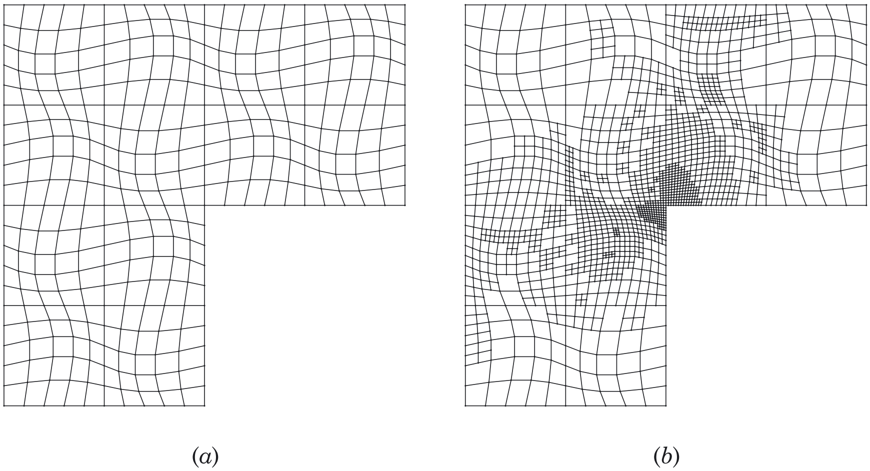

Fig. 2. – The base mesh for both uniform and adaptive calculation, e.g. (a), and the locally refined mesh after three successive adaptive refinements, e.g. (b).

The initial grid adopted in this test is shown in Figure 2(a), and is given by applying the coordinate transformation mapping [12] $(\xi,\zeta)\rightarrow(x,y)$

$$x = \xi + \phi \sin(2\pi\xi)\sin(2\pi\zeta), \tag{33}$$

$$y = \zeta + \phi \sin(2\pi\xi)\sin(2\pi\zeta). \tag{34}$$

with distortion parameter $\phi = 1/10$ to a regular grid of squares in the coordinates system (ξ,ζ).

It is easy to check that, although the load is regular, the exact solution p is only in $H^{5/3}(\Omega)$ due to the presence of the re-entrant corner. Moreover, again due to the non convexity of the domain, the problem regularity parameter s of Corollary 2.1 is 2/3. Thus, the expected asymptotic rates of convergence on uniformly refined meshes are

$$\text{err} \sim N^{-1/3}, \quad |||\boldsymbol{F}^I - \boldsymbol{F}_d|||_{X^d} \sim N^{-1/3}, \quad \|p^I - p_d\|_{Q^d} \sim N^{-2/3}. \tag{35}$$

Conversely, a fully successful adaptive strategy should succeed in recovering the optimal convergence rate of regular problems, that is

$$\text{err} \sim N^{-1/2}, \quad |||\boldsymbol{F}^I - \boldsymbol{F}_d|||_{X^d} \sim N^{-1/2}, \quad \|p^I - p_d\|_{Q^d} \sim N^{-1}. \tag{36}$$

First, note that the mesh depicted in Figure 2(b) shows how the adaptive strategy correctly refines near the re-entrant corner. As it can be checked in Figure 3(a)-(c), the numerical results agree with the above predictions. Moreover, Figure 3(d) shows the good behavior of the effectivity index.

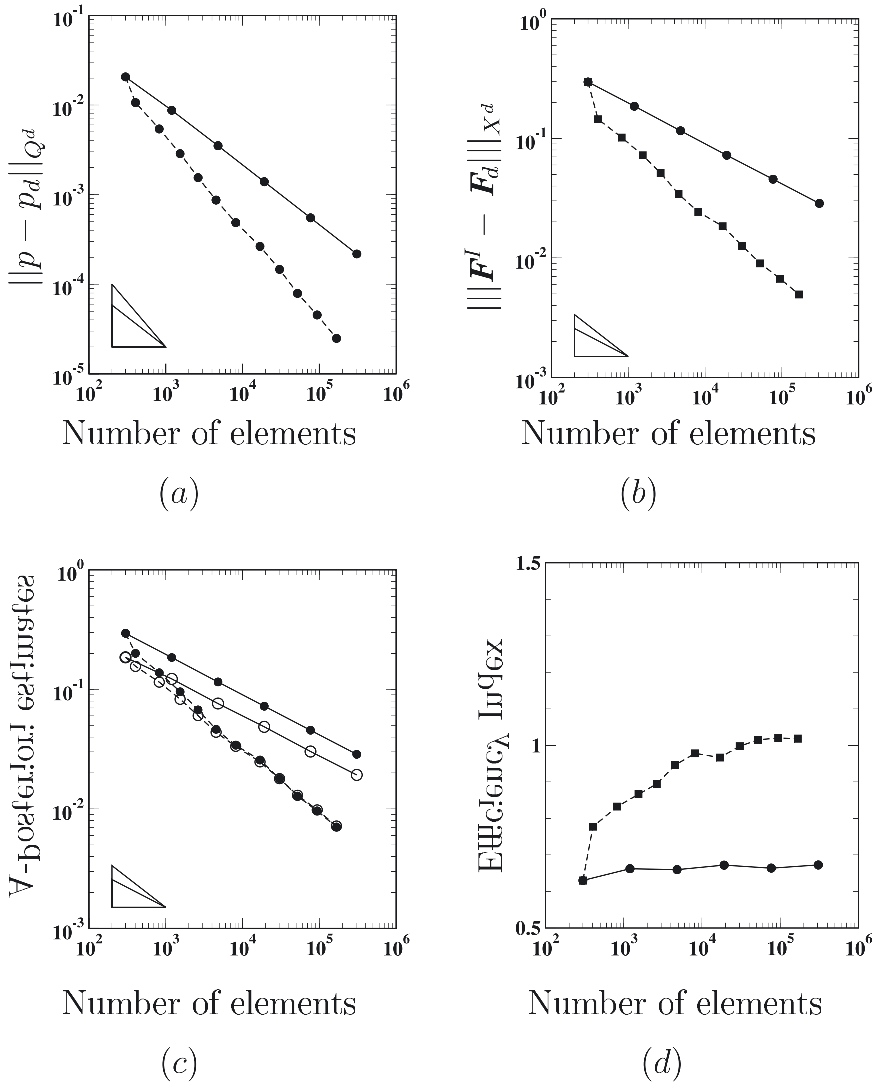

Fig. 3. – Numerical results from uniform (solid lines) and adaptive (dashed lines) calculations; plot (*a*) shows the pressure error in the $|||\cdot|||_{Q^d}$-norm; plot (*b*) shows the flux error in the $|||\cdot|||_{X^d}$-norm; plot (*c*) shows the a-posteriori estimate η (empty circles) and the global error (filled circles); plot (*d*) shows the efficiency index.

REFERENCES

[1] M. AINSWORTH - J. T. ODEN, *A Posteriori Error Estimation in Finite Element Analysis*. Wiley (2000).

[2] S. Agmon, *Lectures on Elliptic Boundary Value Problems*. Van Nostrand, Princeton, NJ (1965).

[3] D. Arnold, *An interior penalty finite element method with discontinuous elements*. SIAM J. Numer. Anal., **19** (1982), 742-760.

[4] L. Beirão da Veiga, *A residual based error estimator for the Mimetic Finite Difference method*, Numer. Math., **108** (2008), 387-406.

[5] L. Beirão da Veiga - M. Manzini, *An a posteriori error estimator for the mimetic finite difference approximation of elliptic problems with general diffusion tensors*, preprint IMATI-CNR 17PV07/17/0 (2007)

[6] M. Berndt - K. Lipnikov - J. D. Moulton - M. Shashkov, *Convergence of mimetic finite difference discretizations of the diffusion equation*. J. Numer. Math., **9** (2001), 253-284.

[7] M. Berndt - K. Lipnikov - M. Shashkov - M. F.Wheeler - I. Yotov, *Superconvergence of the velocity in mimetic finite difference methods on quadrilaterals*. Siam J. Numer. Anal., **43** (2005), 1728-1749.

[8] D. Braess - R. Verfürth, *A posteriori error estimators for the Raviart-Thomas element*. Siam. J. Numer. Anal., **33** (1996), 2431-2444.

[9] S. C. Brenner - L. R. Scott, *The Mathematical Theory of Finite Element Methods*. Springer-Verlag (1994).

[10] F. Brezzi - M. Fortin, *Mixed and Hybrid Finite Element Methods*. Springer-Verlag, New York (1991).

[11] F. Brezzi - K. Lipnikov - M. Shashkov, *Convergence of Mimetic Finite Difference Method for Diffusion Problems on Polyhedral Meshes*. SIAM J. Num. Anal., **43** (2005), 1872-1896.

[12] F. Brezzi - K. Lipnikov - V. Simoncini, *A family of mimetic finite difference methods on polygonal and polyhedral meshes*. Math. Models Methods Appl. Sci., **15** (2005), 1533-1553.

[13] F. Brezzi - K. Lipnikov - M. Shashkov, *Convergence of Mimetic Finite Difference Methods for Diffusion Problems on Polyhedral Meshes with curved faces*. Math. Models Methods Appl. Sci., **16** (2006), 275-298.

[14] F. Brezzi - K. Lipnikov - M. Shashkov - V. Simoncini, *A new discretization methodology for diffusion problems on generalized polyhedral meshes*. To appear on Comp. Meth. and Appl. Mech. Engrg.

[15] A. Cangiani - G. Manzini, *Flux reconstruction and pressure post-processing in mimetic finite difference methods. Comput.* Meth. Appl. Mech. Engrg., **197** (2008), 933-945.

[16] C. Carstensen, *A posteriori error estimate for the mixed finite element method*. Math. of Comp., **66** (1996), 465-476.

[17] P. G. Ciarlet, *The Finite Element Method for Elliptic Problems*. North-Holland (1978).

[18] G. Girault - P. Raviart, *Finite Element Methods for Navier-Stokes Equations*. Theory and Algorithms. Springer-Verlag (1986).

[19] J. Hyman - M. Shashkov - M. Steinberg, *The numerical solution of diffusion problems in strongly heterogeneus non-isotropic materials*. J. Comput. Phys., **132** (1997), 130-148.

[20] Y. Kuznetsov - K. Lipnikov - M. Shashkov, *The mimetic finite difference method on polygonal meshes for diffusion-type problems*. Comput. Geosci., 8 (2005), 301-324.

[21] K. Lipnikov - J. Morel - M. Shashkov, *Mimetic finite difference methods for diffusion equations on non-orthogonal non-conformal meshes*. J. Comput. Phys., **199** (2004), 589-597.

[22] K. LIPNIKOV - M. SHASHKOV - D. SVYATSKIY, *The mimetic finite difference discretization of diffusion problem on unstructured polyhedral meshes*. J. Comput. Phys., **211** (2006), 473-491.

[23] R. LISKA - M. SHASHKOV - V. GANZA, *Analysis and optimization of inner products for mimetic finite difference methods on triangular grid*. Math. and Comp. in Simulation, **67** (2004), 55-66.

[24] C. LOVADINA - R. STENBERG, *Energy norm a posteriori error estimates for mixed finite element methods*. Math. Comp., **75** (2006), 1659-1674.

[25] J. MOREL - M. HALL - M. SHASKOV, *A local support-operators diffusion discretization scheme for hexahedral meshes*. J. of Comput. Phys., **170** (2001), 338-372.

[26] J. MOREL - R. ROBERTS - M. SHASHKOV, *A local support-operators diffusion discretization scheme for quadrilateral r - z meshes*. J. of Comput. Phys., **144** (1998), 17-51.

[27] R. STENBERG, *Postprocessing schemes for some mixed finite elements*. Math. Model. and Numer. Anal., **25** (1991), 151-168.

[28] R. VERFÜRTH, *A review of a posteriori error estimation and adaptive mesh refinement*. Wiley and Teubner, Stuttgart (1996).

Dipartimento di Matematica “F. Enriques”,
Via Saldini 50, 20133 Milano, Italia
e-mail: beirao@mat.unimi.it

Received January 15, 2008 and in revised form February 1, 2008